

# Oscillator strength measurements in Pr II with the fast-ion-beam laser-induced-fluorescence technique

**R Li<sup>1</sup>, R Chatelain<sup>2</sup>, R A Holt<sup>1</sup>, S J Rehse<sup>3</sup>, S D Rosner<sup>1</sup> and T J Scholl<sup>1</sup>**

<sup>1</sup> Department of Physics and Astronomy, University of Western Ontario, London, ON, N6A 3K7, Canada

<sup>2</sup> Department of Physics, McGill University, Montréal, QC, H3A 2T8, Canada

<sup>3</sup> Department of Physics and Astronomy, Wayne State University, Detroit, MI, 48202, USA

E-mail: [rosner@uwo.ca](mailto:rosner@uwo.ca)

Received 25 May 2007

Accepted for publication 10 September 2007

Published 16 October 2007

Online at [stacks.iop.org/PhysScr/76/577](http://stacks.iop.org/PhysScr/76/577)

## Abstract

The spontaneous-emission branching fractions of 32 levels of Pr II were measured by the fast-ion-beam laser-induced-fluorescence technique. The levels studied had energies from  $\sim 21\,500$  to  $\sim 29\,000\text{ cm}^{-1}$ , and the decay branches detected were in the range from 250 to 850 nm. The experimental uncertainties are within 10%. Using our previously measured radiative lifetimes, we determined the Einstein *A* coefficients and oscillator strengths for 260 transitions. The results are important for stellar elemental abundance determinations.

PACS numbers: 32.70.Cs, 32.70.Fw, 95.30.Ky

## 1. Introduction

The study of lanthanide (rare-earth) elements in stellar photospheres is important in increasing our understanding of nucleosynthesis, and the mechanisms which move elements between the core of a star and its surface. The lanthanides are particularly useful because they constitute a continuous sequence of atomic numbers, and their spectra fall in similar wavelength ranges, yet the nucleosynthesis pathways leading to the formation of the many different stable isotopes can be quite different. In his extensive review of the lanthanide elements in stellar spectra [1], Wahlgren pointed out the importance of metal-poor galactic halo stars in testing models of nucleosynthesis that proceed via the *r*- (rapid) and *s*- (slow) neutron capture processes. In a recent study of these stars, abundances of singly-ionized La, Eu, Dy and Nd were used to infer an inhomogeneous distribution of neutron-capture elements in the early interstellar medium [2]. Lanthanide elements are also found in the Sun, and in chemically peculiar (CP) stars of the upper main sequence, where their abundance is high compared to solar values. In CP stars with measurable magnetic-field effects, the abundances of the lanthanide elements are among the most enhanced. Strasser *et al* [3] have studied the strengths and line profiles of Pr, Nd, and other elements in the slowly rotating Ap star HD 187474 in order to model their abundance distributions over the stellar

surface and test a previously derived magnetic field geometry. Lanthanides are also important in the comparison of solar and meteoritic elemental abundances, which have often been taken to be the same [4].

Laboratory measurement of oscillator strengths (*f*-values) is of prime importance in inferring abundances. As astrophysical models become more detailed, improving the accuracy of *f*-values becomes more important. For example, it is expected that systematic differences between solar and meteoritic abundances should exist because of selective diffusion of elements to and from the visible photosphere, but higher accuracy is required to observe this effect [4].

In the 1930s, Meggers *et al* began a program of intensity measurements at the US National Bureau of Standards that led to a number of monographs listing intensities [5, 6] and oscillator strengths [7]. The accuracy of the oscillator strengths was limited by the assumptions about local thermodynamic equilibrium, rate of entry and exit of atoms from the discharge, and negligible self-absorption. The overall uncertainty in  $\log gf$  (where *f* is the absorption oscillator strength and *g* is the multiplicity  $2J+1$  of the lower state) was estimated as a standard deviation varying from 0.24 to 0.29 as the upper-level term energy varied from  $1.5 \times 10^4$  to  $5.0 \times 10^4\text{ cm}^{-1}$ , corresponding to a factor of error of 1.7–2.0 in *gf*.

A more accurate approach to determining oscillator strengths is to combine data on the branching fractions (BFs) for all transitions from a given level with a value for the spontaneous emission lifetime of that level. Lage and Whaling [8] measured BFs in a hollow-cathode discharge and incorporated the beam-foil lifetime measurements of Andersen and Sorensen [9] to obtain oscillator strengths for transitions from five levels of Pr II. Kurucz and Bell [10] have compiled experimental oscillator strengths in a form which is available online (<http://cfa-www.harvard.edu/amp/ampdata/kurucz23/sekur.html>) using the data of Lage and Whaling, BFs from the intensity measurements of Meggers *et al*, together with experimental lifetime data. Goly *et al* [11] obtained BF values for 62 Pr II transitions by measuring the emission from a ferroelectric plasma source. Using Fourier transform spectrometry and previously measured lifetimes, Ivarsson *et al* [12] determined oscillator strength values for 31 lines of Pr II in the 280–800 nm range. Biémont *et al* [13] performed relativistic Hartree–Fock (HFR) calculations of BFs for 24 levels and combined them with their own time-resolved laser-induced-fluorescence lifetime measurements to calculate oscillator strengths for  $\sim 150$  transitions; these are available online from the DREAM database (<http://w3.umh.ac.be/~astro/dream.shtml>).

In the present work, we have carried out a measurement of BFs of Pr II for all levels whose lifetimes we determined in a previous study [14]. The use of a laser/fast-ion-beam method enables highly selective excitation of ions to the level of interest. The resulting uncluttered fluorescence spectrum contains only transitions that emanate from that common upper level, so it is impossible to mistakenly include branches that belong to other upper levels. The combination of the previously measured lifetimes with the BFs measured here produces oscillator strengths with experimental uncertainties of  $\sim 10\%$  arising mainly from the calibration of the optical response of our detector system as a function of wavelength.

## 2. Experimental method

In our apparatus,  $\text{Pr}^+$  ions are produced by surface ionization on a hot tungsten filament in a modified Danfysik 911A source. The ion source contains only Pr vapor produced by a small, electrically heated oven, and there is no discharge. Under such conditions, ions can be produced in metastable states with energies up to several  $1000 \text{ cm}^{-1}$ ; in this work we utilized metastable ions with energies up to  $5079 \text{ cm}^{-1}$ . After acceleration to  $10 \text{ keV}$ , the ions are focused and mass-filtered by a Wien filter before being electrostatically deflected to merge collinearly with a counter-propagating laser beam. The collinear geometry creates kinematic compression [15] of the Doppler width to  $\sim 150 \text{ MHz}$ , which increases the signal size and makes the excitation process more selective. The ion current, typically  $\sim 100 \text{ nA}$ , is detected by a Faraday cup with secondary-electron suppression.

The single-frequency laser beam is produced by an argon-ion-pumped Coherent 699–21 dye laser using Stilbene 3 dye, which has a nominal single-frequency tuning curve from 415 to 465 nm. Given the metastable energy range of the ions, we

can study all excited levels from  $\sim 21\,500$  to  $\sim 29\,000 \text{ cm}^{-1}$  for Pr II, except for some levels whose lifetimes are too long to provide sufficient signal in our detection apparatus. The laser wavelength is determined to  $\sim 1$  part in  $10^7$  with a traveling-mirror Michelson interferometer using a polarization-stabilized reference helium-neon laser as a reference [16, 17].

Ion resonance with the counter-propagating laser beam is confined to a small post-acceleration region. As the ions enter this region, they are accelerated and brought into resonance with the Doppler-shifted laser beam. The excitation occurs primarily in a central cylindrical volume in which the potential is nearly uniform over  $\sim 3 \text{ cm}$  length. The background light from scattered laser light is reduced by focusing the laser beam and the use of apertures, while the light arising from ion-neutral collisions is kept at an acceptable level by maintaining the vacuum at  $10^{-6}$ – $10^{-7}$  Torr. The light background is further suppressed by modulating the post-acceleration potential at  $2 \text{ kHz}$ , providing an ac component to the LIF that is detected with a lock-in amplifier.

Two bundles of optical fibers are positioned around the post-acceleration region to collect the LIF. The LIF from one bundle is used for branching-fraction data while the other provides a ‘normalization’ signal that is used to correct the branching-fraction signal for variations in the excitation rate due to drifts in the properties of the laser and ion beams. This normalization signal is obtained from a relatively strong transition in the LIF spectrum, and is divided into the branching-fraction signal before relative intensities are calculated. The fibers of each bundle are mounted in specific angular arrays chosen to minimize systematic error in the BFs arising from anisotropic excitation and detection [18].

The two fiber bundles are connected to two identical  $f/3.8$  scanning monochromators. Each monochromator has three gratings on a rotating carousel to provide complete spectral coverage: their reciprocal linear dispersions and spectral ranges are as follows:  $(1.0 \text{ nm mm}^{-1}, 250\text{--}500 \text{ nm})$ ,  $(1.5 \text{ nm mm}^{-1}, 250\text{--}750 \text{ nm})$ , and  $(3.0 \text{ nm mm}^{-1}, 250\text{--}1500 \text{ nm})$ . The light detector for the normalization monochromator is a bialkali-photocathode blue-sensitive photomultiplier (PMT), while that for the branching-ratio monochromator is a trialkali-photocathode PMT with extended red response useful in practice to  $\sim 850 \text{ nm}$ . In order to eliminate second-order diffraction lines, a long-pass filter (91.5% flat transmission for wavelength  $\lambda > 550 \text{ nm}$ ) is inserted for scans above  $\sim 600 \text{ nm}$ . The PMTs were operated in current mode to allow the use of lock-in detection for background suppression and wavelength stabilization (see below).

To calibrate the wavelength-dependent response of the complete detector system (fibre array + monochromator + PMT), a 200-W NIST-traceable quartz-tungsten-halogen (QTH) lamp (Oriel model 63355) is used as a standard illumination source. The uncertainty of the response calibration was estimated as 7.1% systematic and 1.5% statistical. For a detailed discussion see [18].

The signal from the normalization monochromator is connected to two lock-in amplifiers. One operating in ‘ $2f$ ’ mode provides the background-suppressed normalization signal, while the second, operating in ‘ $1f$ ’ mode, provides an

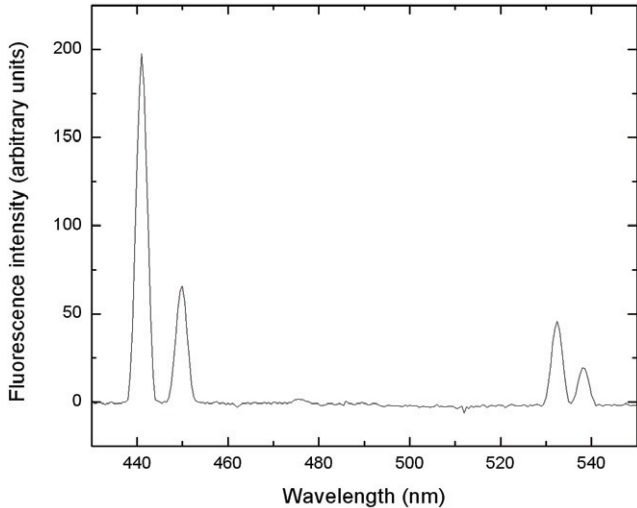


**Figure 1.** Partial fluorescence spectrum in Pr II from the upper level with energy  $22675.439\text{ cm}^{-1}$ . This level was laser-excited using the transition at  $440.88\text{ nm}$  from the ground state of the ion. The laser power was  $115\text{ mW}$  and the ion current is  $75\text{ nA}$ . Dwell time was  $4\text{ s}$  per  $1\text{-nm}$  step.

error signal for dye-laser wavelength stabilization. With the laser wavelength locked to the peak of the pump-transition resonance, the branching-fraction monochromator is scanned to record the spontaneous emission lines from  $250$  to  $850\text{ nm}$ . During a scan, the computer also records the normalization signal, the laser power transmitted through the apparatus, and the ion-beam current. A sample decay-branch partial spectrum for the upper level  $22675.44\text{ cm}^{-1}$  is shown in figure 1.

### 3. Data analysis

BFs are obtained from a spectrum such as that shown in figure 1 by determining the relative intensities of all observed transitions from an excited state. For transitions from an upper state  $u$  to a set of lower states  $l$ , the relative intensities  $I_{ul}$  are obtained by dividing the areas  $S_{ul}$  of the observed spectral lines by the wavelength-dependent detection sensitivity of our apparatus. The latter is determined in a separate calibration procedure employing our QTH irradiance standard as  $r(\lambda_{ul})/i(\lambda_{ul})$ , where  $r(\lambda_{ul})$  is the measured response of our fibre/monochromator/PMT system, and  $i(\lambda_{ul})$  is the value of the manufacturer's spectral irradiance data for our lamp. Altogether,

$$I_{ul} = \frac{S_{ul}}{[r(\lambda_{ul})/i(\lambda_{ul})]}. \quad (1)$$

BFs  $R_{ul}$  are then obtained as

$$R_{ul} = \frac{I_{ul}\lambda_{ul}}{\sum_l I_{ul}\lambda_{ul}}, \quad (2)$$

in which the  $\lambda_{ul}$  factors are needed to convert relative intensities into relative photon emission rates.

The areas  $S_{ul}$  are found by least-squares fitting the emission lines with a symmetric Gaussian function, chosen after a systematic study to optimize goodness of fit and robustness [18]. The uncertainties associated with the areas obtained from the fitting procedure ranged from  $0.2\%$  for the

strongest lines to  $5\%$  for the weakest. Due to the wavelength-dependent dispersion of a Czerny–Turner monochromator, a linewidth function  $w(\lambda) = A(\lambda - \bar{\lambda})^2 + B(\lambda - \bar{\lambda}) + C$  was employed in the fitting, where  $\bar{\lambda}$  is the mean wavelength of the scanned range (introduced merely to reduce correlation between the fitted parameters and minimize truncation errors). This quadratic parameterization was a satisfactory representation of the true wavelength dependence over the range of interest, and provided a robust fit for small peaks common in the infrared region for Pr II.

In some cases it is necessary to combine partial spectra taken with different gratings in order to obtain complete spectral coverage with adequate resolution. The relative normalization of the spectra being combined is determined from spectral lines in the overlap regions common to both spectra. The procedure employs a least-squares adjustment of  $n - 1$  multiplicative normalization constants when the fitted areas from  $n$  spectra are being merged.

### 4. Results

The data required for the BF calculation are the relative intensities of all measured branches from a given upper state. These data are presented in table 1. Obtaining BFs from relative intensities assumes that all radiative transitions that contribute to the decay of the level have been measured. This is practically impossible due to the limited spectral region of detectors and poor signal-to-noise ratio (SNR) for a number of weak lines, predominantly in the near infrared region. (In both tables 1 and 2, lines labeled as ‘w’ were reproducible to the eye but could not be fit because of a poor SNR.) In our work, only the transitions between  $250$  and  $850\text{ nm}$  were observed, and the  $gA$  and  $\log gf$  values derived from them are presented in table 2, along with  $gA$  values from [8, 11–13] where available. To assess the error in our  $gA$  values arising from unseen branches, it is interesting to compare our data with that of Ivarsson *et al* [12], who also measured both lifetimes and BFs but made a theoretical correction for missed branches. Except for the upper level at  $22675.44\text{ cm}^{-1}$ , the agreement is almost always excellent, implying that the contribution of missed branches is comparable with the experimental uncertainties. For the same  $22675.44\text{ cm}^{-1}$  upper level, the agreement between the data of Goly *et al* [11] and our work is excellent (except for one branch where they took data from elsewhere), and our spectrum has a very good SNR, so the disagreement with Ivarsson *et al* on this level is puzzling. It is interesting to note that for the upper level at  $26860.44\text{ cm}^{-1}$ , three branches are in excellent agreement (difference  $<1$  standard deviation), while the branch at  $426.179\text{ nm}$  gives very poor agreement (difference  $>6$  standard deviations). Since this line is listed as ‘complex’ by Meggers *et al* [6], it is likely that Ivarsson *et al* measured a blend in their hollow cathode discharge, while we observed a single line because of our selective laser excitation of the upper level.

In table 3, we make an overall numerical comparison of our results for  $g_u A_{ul}$  to those of [11, 12], both of whom used measured lifetimes and measured BFs, and gave error estimates. For these references we list the average quantity

**Table 1.** Relative intensities of branches from a given upper level of Pr II. The intensities of branches that were observed but too weak to analyze are indicated by 'w'.

Upper level energy <sup>a</sup> (cm <sup>-1</sup> )	Lower level energy <sup>a</sup> (cm <sup>-1</sup> )	Wavelength in air <sup>b</sup> (nm)	Relative intensity
22040.05	0.00	453.592 <sup>c</sup>	1
	441.95	462.874	0.69(8)
	1649.01	490.275 <sup>d</sup>	0.17(2)
	1743.72	492.563 <sup>d</sup>	
	3403.21	536.423	0.011(5)
	3893.46	550.915	0.36(4)
	4097.60	557.183	0.16(2)
	7438.23	684.659 <sup>d</sup>	0.05(2)
	7446.43	685.046 <sup>d</sup>	
22571.48	0.00	442.913 <sup>c</sup>	1
	441.95	451.758	0.27(3)
	1649.01	477.822 <sup>d</sup>	0.072(8)
	1743.72	479.994 <sup>d</sup>	
	3403.21	521.551	0.034(5)
	3893.46	535.240	0.32(3)
	4097.60	541.154	0.14(1)
22675.44	0.00	440.882 <sup>c</sup>	1
	441.95	449.646	0.36(4)
	3893.46	532.276	0.36(4)
	4097.60	538.126	0.16(2)
	7438.23	656.107 <sup>d</sup>	0.05(1)
	7446.43	656.462 <sup>d</sup>	
22885.59	0.00	436.833 <sup>c</sup>	1
	441.95	445.436	0.13(1)
	1649.01	470.754	0.10(1)
	1743.72	472.863	0.11(1)
	3403.21	513.142	0.031(5)
	3893.46	526.388	0.32(3)
	4097.60	532.107	0.13(1)
	7438.23	647.181 <sup>d</sup>	0.032(8)
	7446.43	647.526 <sup>d</sup>	
23261.36	0.00	429.777 <sup>c</sup>	1
	441.95	438.101	0.036(5)
	1743.72	464.605	0.15(2)
	3403.21	503.432	0.023(5)
	3893.46	516.174	0.30(3)
	4097.60	521.673	0.08(1)
	7438.23	631.813	w
	8099.72	659.374 <sup>e</sup>	0.008
23660.20	0.00	422.535 <sup>c</sup>	1
	441.95	430.576	0.34(4)
	4097.60	511.038	0.14(2)
	7438.23	616.278	w
	7446.43	616.594	w
	7744.27	628.128	w
23977.83	441.95	424.763 <sup>c</sup>	1
	1649.01	447.726	0.45(6)
	1743.72	449.634	0.52(7)
	2998.36	476.523	0.20(3)
	3403.21	485.900	0.13(2)
	5108.40	529.809	0.66(8)
	5226.52	533.148	0.23(3)
	8489.87	645.484	w
	10030.31	716.777	w
24115.50	441.95	422.293 <sup>c</sup>	1
	1649.01	444.983	0.27(5)
	1743.72	446.866	0.47(8)
	2998.36	473.42	0.11(2)
	3403.21	482.670	w

**Table 1.** Continued.

Upper level energy <sup>a</sup> (cm <sup>-1</sup> )	Lower level energy <sup>a</sup> (cm <sup>-1</sup> )	Wavelength in air <sup>b</sup> (nm)	Relative intensity
	3893.46	494.372	w
	5079.35	525.17 <sup>d</sup>	0.36(4)
	5108.40	525.973 <sup>d</sup>	
	5226.52	529.262	0.16(2)
	6413.93	564.765	w
	8489.87	639.796	w
24393.73	1743.72	441.377 <sup>c</sup>	1
	3403.21	476.272	0.27(3)
	4097.60	492.567	w
	5108.40	518.385	0.20(2)
	5226.52	521.580	0.048(7)
	8465.04	627.625 <sup>d</sup>	0.008(3)
	8489.87	628.605 <sup>d</sup>	
	10163.47	702.534	0.028(5)
	11418.52	770.498	0.047(9)
24716.04	0	404.481	0.36(4)
	441.95	411.846	1
	1649.01	433.397	0.4(1)
	1743.72	435.184 <sup>c</sup>	0.6(2)
	3893.46	480.114	w
	5226.52	512.952	0.25(3)
	7438.23	578.617	w
	7446.43	578.892	w
	8099.72	601.648	w
	8489.87	616.118	0.13(3)
	9128.67	641.368	w
24835.03	441.95	409.840	0.18(2)
	1743.72	432.941 <sup>c</sup>	1
	2998.36	457.817	0.32(3)
	3403.21	466.465	0.76(8)
	5079.35	506.043 <sup>d</sup>	0.12(2)
	5108.40	506.788 <sup>d</sup>	
	6413.93	542.705	0.05(1)
	9646.67	658.218	0.034(6)
	10163.47	681.404	0.10(1)
	10535.83	699.147	0.031(6)
	11418.52	745.145 <sup>d</sup>	0.041(8)
	11447.73	746.771 <sup>d</sup>	
25248.69	1649.01	423.615 <sup>c</sup>	1
	2998.36	449.306	0.19(2)
	3403.21	457.632	0.34(4)
	4437.15	480.369	0.055(7)
	5079.35	495.664	0.62(6)
	6417.83	530.896	0.17(2)
	11749.49	740.581	0.04(3)
	11794.38	743.052	0.05(1)
	12243.49	768.712	0.03(1)
	13029.09	818.134	0.04(3)
25467.47	0.00	392.547	0.53(6)
	441.95	399.479	1
	1743.72	421.400 <sup>c</sup>	0.022(3)
	4097.60	467.818	0.031(4)
	7438.23	554.501 <sup>d</sup>	0.074(8)
	7446.43	554.753 <sup>d</sup>	
	8099.72	575.617	0.11(1)
	9045.00	608.752	0.09(1)
25499.52	0	392.053	0.25(4)
	441.95	398.968	1
	1649.01	419.160	0.68(9)

**Table 1.** Continued.

Upper level energy <sup>a</sup> (cm <sup>-1</sup> )	Lower level energy <sup>a</sup> (cm <sup>-1</sup> )	Wavelength in air <sup>b</sup> (nm)	Relative intensity
	1743.72	420.832 <sup>c</sup>	0.47(6)
	3403.21	452.438	0.025(4)
	3893.46	462.704	0.034(5)
	5226.52	493.130	0.017(3)
	7438.12	553.517 <sup>d</sup>	0.13(2)
	7446.43	553.768 <sup>d</sup>	
	8099.72	574.560	0.022(4)
	8465.04	586.883	0.10(1)
	9128.67	610.672	0.035(5)
	10116.63	649.893	0.03(1)
	10163.47	651.879	0.04(2)
25569.19	1649.01	417.939	1
	2998.36	442.925 <sup>c</sup>	0.26(3)
	3403.21	451.015	0.27(3)
	5079.35	487.91 <sup>d</sup>	0.020(6)
	5108.4	488.60 <sup>d</sup>	
	5226.52	491.440	w
	6413.93	521.905 <sup>d</sup>	0.45(5)
	6417.83	522.011 <sup>d</sup>	
	7659.76	558.210	w
	9646.67	627.868	w
25610.20	441.95	397.214	0.79(8)
	1649.01	417.225	1
	1649.01	417.225	1
	2998.36	442.122 <sup>c</sup>	0.23(2)
	3403.21	450.182	0.047(6)
	5079.35	486.936 <sup>d</sup>	0.056(6)
	5108.4	487.626 <sup>d</sup>	
	6413.93	520.790	0.19(2)
	8465.04	583.094 <sup>d</sup>	0.065(7)
	8489.87	583.939 <sup>d</sup>	
	9378.63	615.910	0.030(3)
	9646.67	626.255	0.046(5)
	10535.83	663.195	0.011(2)
	11418.52	704.445	0.021(3)
25656.69	441.95	396.481	0.9(1)
	1649.01	416.416	1
	1743.72	418.065 <sup>e</sup>	0.038
	2998.36	441.215 <sup>c</sup>	0.08(2)
	3403.21	449.242	0.025(5)
	5079.35	485.836 <sup>d</sup>	0.043(7)
	5108.4	486.523 <sup>d</sup>	
	6413.93	519.531	0.19(2)
	7438.23	548.742	0.010(3)
	8465.05	581.517 <sup>d</sup>	0.07(1)
	8489.87	582.358 <sup>d</sup>	
	9378.63	614.151	0.018(3)
	9646.67	624.435	0.035(5)
	11418.52	702.151	0.036(6)
26146.01	0	382.359	0.08(1)
	441.95	388.934	0.49(5)
	1649.01	408.098	0.65(7)
	1743.72	409.682	1
	3403.21	439.576 <sup>c</sup>	0.06(1)
	3893.46	449.261	0.020(5)
	7438.23	534.388 <sup>d</sup>	0.08(1)
	7446.43	534.623 <sup>d</sup>	
	8465.04	565.423	0.07(2)
	8489.87	566.219	0.02(1)
	9128.67	587.474	0.037(6)

**Table 1.** Continued.

Upper level energy <sup>a</sup> (cm <sup>-1</sup> )	Lower level energy <sup>a</sup> (cm <sup>-1</sup> )	Wavelength in air <sup>b</sup> (nm)	Relative intensity
26398.52	10163.47	625.510	0.045(7)
	10729.75	648.487	0.011(3)
26445.11	441.95	385.155	0.24(3)
	1649.01	403.934	0.29(3)
	1743.72	405.488	1
	2998.36	427.227	0.35(4)
	3403.21	434.749 <sup>c</sup>	0.24(3)
	6413.93	500.246	0.044(8)
	7438.23	527.271	w
	8465.04	557.461 <sup>d</sup>	0.005(2)
	8489.87	558.235 <sup>d</sup>	
	9378.63	587.383	0.009(3)
	9646.67	596.782	0.046(8)
	10163.47	615.782	0.008(3)
	10535.83	630.236	0.014(4)
	11418.52	667.378	0.06(1)
	11794.38	684.547	w
26524.02	1649.01	403.175	1
	2998.36	426.378	0.33(3)
	3403.21	433.870 <sup>c</sup>	0.44(5)
	4437.15	454.254	0.048(6)
	5079.35	467.908 <sup>d</sup>	0.13(1)
	5108.4	468.545 <sup>d</sup>	
	6413.93	499.083 <sup>d</sup>	0.075(8)
	6417.83	499.180 <sup>d</sup>	
	7659.76	532.182	0.13(1)
	9646.67	595.127	0.010(3)
	10030.31	609.038	0.07(1)
	11005.57	647.509	0.014(4)
	11749.49	680.287 <sup>d</sup>	0.025(6)
	11794.38	682.372 <sup>d</sup>	
	13029.09	745.174	0.08(1)
26640.86	441.95	383.296	0.42(4)
	1743.72	403.433	1
	2998.36	424.948 <sup>c</sup>	0.39(4)
	3403.21	432.390	0.23(2)
	6413.93	497.125	0.038(5)
	8465.04	553.588 <sup>d</sup>	0.026(5)
	8489.87	554.350 <sup>d</sup>	
	9646.67	592.346	0.066(8)
	10535.83	625.289	0.031(7)
	11418.52	661.834	0.16(2)
26707.31	1649.01	400.017	0.71(8)
	1743.72	401.539	1
	3403.21	430.215 <sup>c</sup>	0.12(2)
	9378.63	579.136	0.13(2)
	9646.67	588.274	0.04(1)
	10116.63	605.004	0.10(3)
	10163.47	606.727	0.07(2)
	0	374.323	0.020(3)
	441.95	380.622	0.028(4)
	1743.72	400.470	1
	3403.21	428.988 <sup>c</sup>	0.14(2)

5226.52 465.402 0.029(3)

7438.23 518.822<sup>d</sup> 0.048(5)7446.43 519.043<sup>d</sup>

8099.72 537.266 0.005(2)

8465.04 548.026<sup>d</sup> 0.033(4)8489.87 548.772<sup>d</sup>

9821.67 568.717 0.011(3)

**Table 1.** Continued.

Upper level energy <sup>a</sup> (cm <sup>-1</sup> )	Lower level energy <sup>a</sup> (cm <sup>-1</sup> )	Wavelength in air <sup>b</sup> (nm)	Relative intensity
	9378.63	576.916	0.051(6)
	10163.47	604.287	0.09(1)
26860.95	1649.01	396.525	0.66(7)
	2998.36	418.948 <sup>c</sup>	1
	3403.21	426.179	0.037(5)
	4437.15	445.830	0.047(6)
	5108.40	459.588	w
	6413.93	488.933 <sup>d</sup>	0.043(5)
	6417.83	489.026 <sup>d</sup>	
	7659.76	520.655	0.17(2)
	8140.67	534.032	w
	9646.67	580.752	0.009(2)
	10030.31	593.990	0.08(1)
	10163.47	598.729	w
	10729.75	619.745	0.019(3)
	11005.57	630.523	0.014(2)
	13029.09	722.770	0.017(3)
26961.96	441.95	376.967	w
	1649.01	394.943	1
	1743.72	396.426	0.85(9)
	2998.36	417.182	0.93(10)
	3403.21	424.351 <sup>c</sup>	0.33(4)
	5079.35	456.856	w
	6413.93	486.529	w
	8465.04	540.480 <sup>d</sup>	0.026(9)
	8489.87	541.207 <sup>d</sup>	
	9378.63	568.560	0.023(8)
	10030.31	590.445	0.09(2)
	10163.47	595.127	0.10(2)
	10535.83	608.616	0.04(1)
	11418.52	643.184 <sup>d</sup>	0.11(3)
	11447.73	644.391 <sup>d</sup>	
27128.00	2998.36	414.311	1
	4437.15	440.583 <sup>c</sup>	0.18(2)
	5079.35	453.415 <sup>d</sup>	0.10(1)
	5108.40	454.014 <sup>d</sup>	
	6413.93	482.629	w
	6417.83	482.720	w
	7659.76	513.514	0.11(1)
	7805.61	517.390	0.29(3)
	8958.49	550.220	w
	10030.31	584.713	0.05(1)
	11005.57	620.081	w
	11611.05	644.278	w
27781.69	2998.36	403.383	1
	4437.15	428.242 <sup>c</sup>	0.72(7)
	5079.35	440.360	0.31(3)
	7805.61	500.459	0.08(1)
	8958.49	531.112	0.14(2)
	11611.05	618.234	0.08(1)
	14705.96	764.566	0.013(8)
28009.80	1649.01	379.244	0.11(2)
	2998.36	399.704	0.30(3)
	3403.21	406.281	1
	4437.15	424.101 <sup>c</sup>	0.45(5)
	5079.35	435.979 <sup>d</sup>	0.17(2)
	5108.40	436.532 <sup>d</sup>	
	7659.76	491.26	0.06(1)
	11005.57	587.925	0.09(1)

**Table 1.** Continued.

Upper level energy <sup>a</sup> (cm <sup>-1</sup> )	Lower level energy <sup>a</sup> (cm <sup>-1</sup> )	Wavelength in air <sup>b</sup> (nm)	Relative intensity
	11749.49	614.824 <sup>d</sup>	0.05(1)
	11794.38	616.527 <sup>d</sup>	
	12826.94	658.456	w
	13029.09	667.341	0.09(2)
	13373.61	683.050	w
28034.08	2998.36	399.316	0.18(2)
	3403.21	405.880	1
	5079.35	435.518 <sup>c</sup>	0.29(4)
	5108.40	436.070 <sup>d</sup>	0.05(2)
	5226.52	438.328 <sup>d</sup>	
	10729.75	577.729	0.11(2)
28172.96	2998.36	397.116	0.35(4)
	3403.21	403.605	0.20(3)
	4437.15	421.186	1
	5079.35	432.899 <sup>c</sup>	0.67(7)
	11749.49	608.717 <sup>d</sup>	0.18(4)
	11794.38	610.385 <sup>d</sup>	
28201.95	2998.36	396.657	0.43(5)
	4437.15	420.672	1
	5079.35	432.355 <sup>c,d</sup>	0.11(2)
	5108.40	432.900 <sup>d</sup>	
	6413.93	458.840 <sup>d</sup>	0.04(2)
	6417.83	458.922 <sup>d</sup>	
	7805.61	490.147	0.05(1)
	8958.49	519.511	0.17(2)
	11005.57	581.355	0.024(8)
	11611.05	602.572	0.10(2)
	11794.38	609.306	
	12243.49	626.454	0.023(9)
	14705.96	740.757	w
28577.79	2998.36	390.829	0.41(5)
	3403.21	397.116	0.32(4)
	4437.15	414.122	1
	5079.35	425.440 <sup>c,d</sup>	0.16(2)
	5108.40	425.967 <sup>d</sup>	
	7659.76	477.923	w
	10729.75	560.130 <sup>d</sup>	0.04(2)
	11005.57	568.921 <sup>d</sup>	
	11611.05	589.225	w
	11749.49	594.072 <sup>d</sup>	0.16(4)
	11794.38	595.660 <sup>d</sup>	
	12826.94	634.711 <sup>d</sup>	0.09(2)
	13029.09	642.963 <sup>d</sup>	

<sup>a</sup>NIST Atomic Spectroscopy Database  
(<http://physics.nist.gov/PhysRefData/ASD/index.html>).

<sup>b</sup>Wavelength sources in order of decreasing priority:

1. NIST Atomic Spectroscopy Database (see footnote a);
2. Kurucz R L and Bell B 1995 Atomic Line Data, Kurucz CD-ROM no. 23 (Cambridge, MA.: Smithsonian Astrophysical Observatory). Online at <http://cfa-www.harvard.edu/amdata/ampdata/kurucz23/sekur.html>;
3. Ritz wavelengths calculated from NIST energy levels.

<sup>c</sup>Transition used to excite the upper level.

<sup>d</sup>Blended line in this work.

<sup>e</sup>Transition observed by [6], but not in this work. The relative intensity is calculated from data in that reference.

**Table 2.** Transition probabilities and oscillator strengths for Pr II derived from branching-fraction and lifetime data. Values of  $g_u A_{ul}$  from this work are compared with those of [8, 11–13]. Branches that were observed but were too weak to fit are indicated by ‘w’.

Upper level energy (cm <sup>-1</sup> ) <sup>a</sup>	<i>J</i>	Lifetime (ns) <sup>b</sup>	Transition wavelength (nm)	Branching fraction	This work	BLQSX <sup>c</sup>	$\frac{g_u A_{ul}}{(10^6 \text{ s}^{-1})}$ ILW <sup>d</sup>	GKNW <sup>e</sup>	LW <sup>f</sup>	$\log g_l f_{lu}$ This work
22040.05	5	67.5(1.7)	453.592	0.38(2)	62(4)					-0.715
			462.874	0.27(2)	44(3)					-0.849
			490.275 <sup>g</sup>	0.070(7)	11(1)					-1.382
			492.563 <sup>g</sup>							
			536.423	0.005(2)	0.8(3)					-2.465
			550.915	0.17(1)	27(2)					-0.903
			557.183	0.073(8)	12(1)					-1.255
			684.659 <sup>g</sup>	0.03(1)	5(1)					-1.469
			685.046 <sup>g</sup>							
22571.48	5	51.8(6)	442.913	0.51(2)	109(5)					-0.495
			451.758	0.14(1)	30(2)					-1.032
			477.822 <sup>g</sup>	0.040(4)	8.5(8)					-1.532
			479.994 <sup>g</sup>							
			521.551	0.021(2)	4.4(5)					-1.750
			535.240	0.20(1)	42(3)					-0.739
			541.154	0.085(7)	18(1)					-1.100
22675.44	5	13.5(2)	440.882	0.48(2)	394(18)		518(41)	358(89)		0.053
			449.646	0.18(1)	144(11)		178(18)	164(41)		-0.368
			532.276	0.21(1)	170(12)		113(12)	207(52)		-0.123
			538.126	0.096(8)	78(7)		18(2.3)	4(1)		-0.461
			656.107 <sup>g</sup>	0.036(8)	29(6)					-0.723
			656.462 <sup>g</sup>							
22885.59	5	35.0(7)	436.833	0.50(2)	158(7)					-0.346
			445.436	0.068(6)	21(2)					-1.199
			470.754	0.057(7)	18(2)					-1.227
			472.863	0.059(7)	19(2)					-1.206
			513.142	0.018(3)	5.8(8)					-1.639
			526.388	0.20(1)	62(5)					-0.592
			532.107	0.077(7)	24(2)					-0.988
			647.181 <sup>g</sup>	0.024(6)	7(2)					-1.329
			647.526 <sup>g</sup>							
23261.36	5	48.8(1.6)	429.777	0.60(2)	134(7)	96.4				-0.429
			438.101	0.022(3)	5.0(6)	41.7				-1.845
			464.605	0.099(9)	22(2)	15.2				-1.142
			503.432	0.016(3)	3.6(7)	7.22				-1.858
			516.174	0.21(2)	48(4)	25.2				-0.720
			521.673	0.056(6)	13(1)					-1.292
			631.813	w		7.85				
			659.374	w		3.62				
23660.20	4	7.57(15)	422.535	0.66(2)	786(29)		494(123)			0.323
			430.576	0.23(2)	269(21)		153(38)			-0.125
			511.038	0.11(1)	134(13)		98(24)			-0.280
			616.278	w						-0.280
			616.594	w						
			628.128	w						
23977.83	6	36.0(9)	424.763	0.28(2)	103(8)					-0.555
			447.726	0.13(1)	49(4)					-0.834
			449.634	0.16(1)	57(4)					-0.762
			476.523	0.063(6)	23(2)					-1.109
			485.900	0.041(4)	15(2)					-1.282
			529.809	0.24(2)	85(6)					-0.446
			533.148	0.083(8)	30(3)					-0.895
			645.484	w						
			716.777	w						
24115.50	6	7.92(15)	422.293	0.39(2)	642(41)	735	698(49)	445(111)	508	0.235
			444.983	0.11(2)	185(31)	181	225(18)	122(31)	161	-0.261
			446.866	0.20(2)	321(40)	299	270(22)	135(34)	200	-0.017

**Table 2.** Continued.

Upper level energy (cm <sup>-1</sup> )	J	Lifetime (ns) <sup>b</sup>	Transition wavelength (nm)	Branching fraction	This work	BLQSX <sup>c</sup>	$\frac{g_u A_{ul}}{(10^6 s^{-1})}$ ILW <sup>a</sup>	GKNW <sup>e</sup>	LW <sup>c</sup>	$\log g_l f_{lu}$ This work
			473.420	0.049(8)	80(13)	2.20		23(6)	33	-0.571
			482.670					10(5)	13	
			494.372			12.0		9(5)	8	
			525.171 <sup>g</sup>	0.17(2)	286(26)	365	314(25)	204(51)	291	0.072
			525.973 <sup>g</sup>							
			529.262	0.08(1)	128(17)	122	132(13)	100(50)	121	-0.269
			564.765	w					9	
			639.796	w		17.3			25	
24393.73	6	80.9(1.3)	441.377	0.58(2)	94(4)					-0.563
			476.272	0.17(1)	27(2)					-1.034
			492.567	w						
			518.385	0.13(1)	22(2)					-1.062
			521.580	0.033(4)	5.3(7)					-1.664
			627.625 <sup>g</sup>	0.007(2)	1.1(3)					-2.178
			628.605 <sup>g</sup>							
			702.534	0.026(4)	4.2(7)					-1.508
			770.489	0.048(8)	8(1)					-1.164
24716.04	5	6.4(11)	404.481	0.12(1)	207(23)			201(50)	-0.293	
			411.846	0.34(3)	588(57)			475(119)	0.175	
			433.397	0.15(4)	251(71)			301(75)	-0.150	
			435.184	0.22(5)	374(89)			157(39)	0.027	
			480.114					33(8)		
			512.952	0.11(1)	186(23)			141(35)	-0.134	
			578.617	w						
			578.892	w						
			601.648	w						
			616.118	0.07(2)	112(26)					-0.196
			641.368	w						
24835.03	6	92.7(1.2)	409.840	0.058(5)	8.2(7)					-1.686
			432.941	0.35(2)	49(3)					-0.861
			457.817	0.12(1)	17(1)					-1.280
			466.465	0.29(2)	40(2)					-0.884
			506.043 <sup>g</sup>	0.050(5)	7.0(7)					-1.570
			506.788 <sup>g</sup>							
			542.705	0.023(5)	3.2(7)					-1.851
			658.218	0.018(3)	2.6(4)					-1.778
			681.404	0.055(6)	7.7(8)					-1.273
			699.147	0.018(3)	2.5(4)					-1.742
			745.145 <sup>g</sup>	0.025(4)	3.4(6)					-1.543
			746.771 <sup>g</sup>							
25248.69	7	96.6(2.0)	423.615	0.35(2)	54(3)					-0.835
			449.306	0.069(6)	10.7(9)					-1.490
			457.632	0.13(1)	20(2)					-1.202
			480.369	0.022(2)	3.4(4)					-1.933
			495.664	0.25(2)	40(3)					-0.837
			530.896	0.074(6)	11(1)					-1.315
			740.581	0.03(2)	4(3)					-1.478
			743.052	0.031(7)	5(1)					-1.401
			768.712	0.016(9)	2(1)					-1.656
			818.134	0.03(2)	5(3)					-1.336
25467.47	4	11.6(9)	392.547	0.26(2)	206(21)			202(50)	-0.323	
			399.479	0.51(2)	392(35)			458(114)	-0.028	
			421.400	0.012(2)	9(1)					-1.624
			467.818	0.018(2)	14(2)			15.3(2.8)	-1.330	
			554.501 <sup>g</sup>	0.052(5)	40(5)					-0.730
			554.753 <sup>g</sup>							
			575.617	0.078(7)	61(7)					-0.521
			608.752	0.070(7)	54(7)					-0.521
25499.52	5	16.2(4)	392.053	0.08(1)	54(7)			64(16)	-0.907	

**Table 2.** Continued.

Upper level energy (cm <sup>-1</sup> )	<i>J</i>	Lifetime (ns) <sup>b</sup>	Transition wavelength (nm)	Branching fraction	This work	BLQSX <sup>c</sup>	$\frac{g_u A_{ul}}{(10^6 s^{-1})}$		LW <sup>c</sup>	$\log g_l f_{lu}$ This work
							ILW <sup>a</sup>	GKNW <sup>e</sup>		
			398.968	0.08(1)	0.33(2)	221(16)			286(29)	-0.277
			419.160	0.23(2)	158(14)				110(11)	-0.379
			420.832	0.16(1)	110(9)				110(11)	-0.535
			452.438	0.009(1)	6.2(7)					-1.718
			462.704	0.013(1)	8.7(9)					-1.554
			493.130	0.007(1)	4.6(7)					-1.776
			553.517 <sup>g</sup>	0.057(5)	39(3)					-0.752
			553.768 <sup>g</sup>							
			574.560	0.010(2)	7(1)					-1.463
			586.883	0.050(4)	34(3)					-0.759
			610.672	0.017(2)	12(1)					-1.181
			649.893	0.015(5)	10(3)					-1.198
			651.879	0.02(1)	15(9)					-1.011
25569.19	7	6.32(39)	417.939	0.46(2)	1099(84)	1240	1146(69)	809(202)	786	0.459
			442.925	0.13(1)	305(30)	162	268(21)	306(76)	342	-0.048
			451.015	0.14(1)	323(32)	302	311(25)	128(32)	174	-0.007
			487.910 <sup>g</sup>	0.011(3)	26(8)	7.07			27	-1.030
			488.600 <sup>g</sup>			18.3		12.8(3.2)	20	
			491.440	w		9.42			10	
			521.905 <sup>g</sup>	0.26(2)	621(56)	170	217(20)	150(37)	143	0.405
			522.011 <sup>g</sup>			508	486(34)	363(91)	353	
			558.210	w					< 1.5	
			627.868	w		21			39	
25610.20	6	21.1(5)	397.214	0.29(2)	179(12)	24.5				-0.374
			417.225	0.38(2)	237(13)					-0.209
			418.880			350				
			442.122	0.094(7)	58(5)	8.40				-0.770
			450.182	0.020(2)	12(1)	117				-1.437
			486.936 <sup>g</sup>	0.025(2)	15(1)	23.1				-1.258
			487.626 <sup>g</sup>							
			520.790	0.089(7)	55(4)					-0.651
			583.094 <sup>g</sup>	0.035(3)	21(2)					-0.962
			583.939 <sup>g</sup>							
			615.910	0.017(2)	11(1)					-1.221
			626.255	0.026(2)	16(1)					-1.022
			663.195	0.007(1)	4.0(7)	4.35				-1.578
			704.445	0.014(2)	8(1)	13.0				-1.200
25656.69	6	9.05(21)	396.481	0.35(2)	498(34)		560(39)	523(131)		0.069
			416.416 <sup>g</sup>	0.40(2)	569(36)			555(44)	540(135)	0.170
			418.065 <sup>g</sup>							
			441.215	0.033(6)	47(9)		48(5.3)	44(11)		-0.859
			449.242	0.010(2)	15(3)					-1.341
			485.836 <sup>g</sup>	0.020(3)	29(4)					-0.989
			486.523 <sup>g</sup>							
			519.531	0.092(8)	132(12)		125(10)	176(44)		-0.272
			548.742	0.005(2)	8(2)					-1.454
			581.517 <sup>g</sup>	0.041(4)	59(6)					-0.520
			582.358 <sup>g</sup>							
			614.151	0.010(2)	15(3)					-1.075
			624.435	0.021(3)	30(4)					-0.760
			702.151	0.024(4)	34(5)					-0.596
26146.01	5	18.8(1.4)	382.359	0.028(3)	16(2)					-1.449
			388.934	0.17(1)	102(11)					-0.634
			408.098	0.25(2)	144(14)					-0.445
			409.682	0.38(2)	221(20)					-0.255
			439.576	0.026(4)	15(2)					-1.361
			449.261	0.008(2)	5(1)					-1.844
			534.388 <sup>g</sup>	0.039(5)	23(3)					-1.011
			534.623 <sup>g</sup>							
			565.423	0.037(7)	21(5)					-0.988

**Table 2.** Continued.

Upper level energy (cm <sup>-1</sup> )	<i>J</i>	Lifetime (ns) <sup>b</sup>	Transition wavelength (nm)	Branching fraction	This work	BLQSX <sup>c</sup>	$g_u A_{ul}$ (10 <sup>6</sup> s <sub>-1</sub> ) ILW <sup>a</sup>	GKNW <sup>e</sup>	LW <sup>c</sup>	$\log g_l f_{lu}$ This work
26398.52	6	8.19(8)	566.219	0.012(5)	7(3)					-1.458
			587.474	0.020(3)	12(2)					-1.217
			625.510	0.026(4)	15(2)					-1.046
			648.487	0.007(2)	4(1)					-1.618
			385.155	0.095(9)	151(20)					-0.475
			403.934	0.12(1)	188(24)					-0.336
			405.488	0.41(2)	657(72)					0.209
			427.227	0.15(1)	244(32)					-0.175
			434.749	0.10(1)	167(23)					-0.326
			500.246	0.023(4)	36(7)					-0.871
			527.271							
			557.461 <sup>g</sup>	0.003(1)	4(2)					-1.696
			558.235 <sup>g</sup>							
			587.383	0.005(2)	8(3)					-1.369
			596.782	0.028(4)	45(8)					-0.621
			615.782	0.005(2)	8(3)					-1.337
			630.236	0.009(2)	14(4)					-1.076
			667.378	0.041(6)	65(12)					-0.360
			684.547	w						
26445.11	7	26.4(1.4)	403.175	0.38(2)	217(16)					-0.276
			426.378	0.132(9)	75(7)					-0.688
			433.870	0.18(1)	103(9)					-0.538
			454.254	0.021(2)	12(1)					-1.439
			467.908 <sup>g</sup>	0.056(5)	32(3)					-0.984
			468.545 <sup>g</sup>							
			499.083 <sup>g</sup>	0.035(3)	20(2)					-1.126
			499.180 <sup>g</sup>							
			532.182	0.068(5)	38(4)					-0.787
			595.127	0.006(2)	3.4(9)					-1.748
			609.038	0.041(5)	24(3)					-0.883
			647.509	0.009(2)	5(1)					-1.516
			680.287 <sup>g</sup>	0.016(3)	9(2)					-1.200
			682.372 <sup>g</sup>							
			745.174	0.054(8)	31(5)					-0.593
26524.02	6	77(7)	383.296	0.16(1)	26(3)					-1.238
			403.433	0.39(2)	66(7)	34.0				-0.790
			424.948	0.16(1)	27(3)	28.7				-1.130
			432.390	0.095(7)	16(2)	24.8				-1.346
			497.125	0.018(2)	3.1(4)					-1.944
			553.588 <sup>g</sup>	0.014(2)	2.4(5)					-1.965
			554.350 <sup>g</sup>							
			592.346	0.038(4)	6.4(9)					-1.473
			625.289	0.019(4)	3.1(7)					-1.734
			661.834	0.11(1)	18(2)					-0.932
26640.86	5	26.2(2)	400.017	0.30(2)	127(9)					-0.515
			401.539	0.43(2)	180(10)					-0.362
			430.215	0.054(6)	23(2)					-1.199
			579.136	0.08(1)	34(5)					-0.768
			588.274	0.026(8)	11(3)					-1.241
			605.004	0.06(2)	27(6)					-0.836
			606.727	0.04(1)	18(5)					-0.993
26707.31	5	30.0(1.4)	374.323	0.012(2)	4.4(6)					-2.037
			380.622	0.017(2)	6.2(8)					-1.872
			400.470	0.64(2)	234(13)					-0.250
			428.988	0.099(8)	36(3)					-1.000
			465.402	0.021(2)	7.7(9)					-1.599
			518.822 <sup>g</sup>	0.040(4)	15(2)					-1.231
			519.043 <sup>g</sup>							
			537.266	0.004(2)	1.6(7)					-2.157
			548.026 <sup>g</sup>	0.029(3)	10(1)					-1.326

**Table 2.** Continued.

Upper level energy (cm <sup>-1</sup> )	J	Lifetime (ns) <sup>b</sup>	Transition wavelength (nm)	Branching fraction			$g_u A_{ul}$ (10 <sup>6</sup> s <sub>-1</sub> )	GKNW <sup>e</sup>	LW <sup>c</sup>	$\log g_l f_{lu}$ This work
					This work	BLQSX <sup>c</sup>				
26860.95	7	6.69(52)	548.772 <sup>g</sup>							-1.751
			568.717	0.010(2)	3.7(9)					-1.070
			576.916	0.046(5)	17(2)					-0.766
			604.287	0.085(8)	31(3)					0.181
			396.525	0.29(2)	643(64)	307	579(41)	315(78)		0.431
			418.948	0.46(2)	1025(93)	1410	917(64)	452(113)		-0.978
			426.179	0.017(2)	39(5)		155(17)	41(20)		-0.817
			445.830	0.023(2)	51(7)	34.9				-0.739
			459.588							-0.739
			488.933 <sup>g</sup>	0.023(2)	51(6)		23.6			-0.048
			489.026 <sup>g</sup>			220(25)	227	214(17)	119(30)	
			520.655	0.098(8)						-0.198
			534.032							-0.198
			580.752	0.005(1)	12(3)	8.13				-1.211
26961.96	6	11.7(5)	593.990	0.053(7)	120(19)	93.8				-0.779
			598.729			15.9				-0.889
			619.745	0.013(2)	29(5)	34.5				-0.612
			630.523	0.010(1)	29(5)	15.8				-0.553
			722.770	0.014(2)	31(6)	3.31				-0.616
			376.967	w						-0.164
			394.943	0.26(2)	293(22)					-0.230
			396.426	0.22(1)	250(20)					-0.123
			417.182	0.26(2)	288(22)					-1.344
			424.351	0.093(8)	104(10)					-1.319
			456.856	w						-0.702
			486.529	w						-0.612
			540.480 <sup>g</sup>	0.009(3)	10(4)					-0.950
			541.207 <sup>g</sup>							-0.494
			568.560	0.009(3)	10(3)					-0.268
27128.00	8	5.79(13)	590.445	0.034(7)	38(8)					-0.240
			595.127	0.041(8)	46(9)					0.359
			608.616	0.018(5)	20(6)					< 10
			643.184 <sup>g</sup>	0.05(1)	52(12)					-0.049
			644.391 <sup>g</sup>							-0.116
			414.311	0.53(2)	1561(71)	1910	1579(95)	921(230)	991	-0.449
			440.583	0.10(1)	297(25)	124	315(25)	156(39)	153	-0.881
			453.415	0.060(5)	175(16)	103	232(25)	109(54)	83	-0.531
			454.014			6.8(3.4)				-0.595
			482.629			10.4	38(4.9)			-1.104
			482.629	w		10.4	38(4.9)			-0.213
27781.69	8	18.4(6)	482.720			18.7				-0.049
			513.514	0.076(7)	222(22)	214	258(28)	145(36)	212	-0.116
			517.390	0.19(1)	569(44)	616	604(48)	345(86)	541	-0.449
			550.220							-0.531
			584.713	0.038(9)	112(25)	16.8				-0.595
			620.081	w		9.61			31	-0.553
			644.278	w						-0.213
			403.383	0.40(2)	366(23)					-0.881
28009.80	7	6.97(21)	428.242	0.30(2)	278(19)					-0.531
			440.360	0.13(1)	122(10)					-0.595
			500.459	0.038(4)	35(4)					-0.268
			531.112	0.075(8)	70(8)					-0.049
			618.234	0.048(6)	44(6)					-0.213
			764.566	0.010(6)	9(5)					-0.350
			379.244	0.042(6)	91(13)					-0.334
			399.704	0.12(1)	256(23)		333(83)			-0.041
			406.281	0.40(2)	871(53)		506(126)	1500		-0.350
			424.101	0.19(1)	408(33)		174(44)	345		-0.213
			435.979 <sup>g</sup>	0.073(8)	157(17)		63(16)	159		-0.049

**Table 2.** Continued.

Upper level energy (cm <sup>-1</sup> )	<i>J</i>	Lifetime (ns) <sup>b</sup>	Transition wavelength (nm)	Branching fraction	This work	BLQSX <sup>c</sup>	$\frac{g_u A_{ul}}{(10^6 s_{-1})}$ ILW <sup>a</sup>	GKNW <sup>e</sup>	LW <sup>c</sup>	$\log g_l f_{lu}$ This work
			436.532 <sup>g</sup>						15	
			491.260	0.030(4)	65(10)			33(8)	86	0.631
			587.925	0.052(7)	111(15)				114	-0.240
			614.824 <sup>g</sup>	0.029(6)	63(13)					-0.444
			616.527 <sup>g</sup>							
			658.456	w						
			667.341	0.061(9)	131(19)					0.059
			683.050	w						
28034.08	6	48.4(3.0)	399.316	0.10(1)	28(3)					-1.172
			405.880	0.59(2)	158(12)					-0.408
			435.518	0.19(2)	50(6)					-0.850
			436.070 <sup>g</sup>	0.03(1)	8(3)					-1.642
			438.328 <sup>g</sup>							
			577.729	0.09(2)	25(5)					-0.909
28172.96	7	70.6(1.9)	397.116	0.13(1)	29(3)					-1.169
			403.605	0.076(8)	16(2)					-1.401
			421.186	0.41(2)	86(5)					-0.640
			432.899	0.28(2)	59(4)					-0.778
			608.717 <sup>g</sup>	0.10(2)	22(4)					-0.909
			610.385 <sup>g</sup>							
28201.95	8	10.7(6)	396.657	0.20(2)	314(30)		419(42)	235(59)		-0.130
			420.672	0.49(2)	779(57)		967(77)	770(77)		-0.315
			432.355 <sup>g</sup>	0.055(9)	87(15)		98(12)	83(21)		-0.613
			432.900 <sup>g</sup>							
			458.840 <sup>g</sup>	0.021(8)	33(13)					-0.980
			458.922 <sup>g</sup>							
			490.147	0.027(8)	43(12)			39(10)		-0.806
			519.511	0.10(1)	163(20)		190(19)			-0.180
			581.355	0.016(5)	25(8)					-0.892
			602.572 <sup>g</sup>	0.07(1)	117(17)					-0.195
			609.306 <sup>g</sup>							
			626.454	0.017(6)	26(10)					-0.808
			740.757	w						
28577.79	7	7.03(28)	390.829	0.17(1)	361(35)					-0.082
			397.116	0.13(1)	285(29)					-0.171
			414.122	0.44(2)	935(64)					-0.381
			425.440 <sup>g</sup>	0.071(9)	151(19)					-0.386
			425.967 <sup>g</sup>							
			477.923	w						
			560.130 <sup>g</sup>	0.02(1)	51(23)					-0.622
			568.921 <sup>g</sup>							
			589.225							
			594.072 <sup>g</sup>	0.10(2)	219(49)					0.064
			595.660 <sup>g</sup>							
			634.711 <sup>g</sup>	0.06(1)	131(22)					-0.101
			642.963 <sup>g</sup>							

<sup>a</sup> NIST Atomic Spectra Database [Ver. 3.0] available online at <http://physics.nist.gov/PhysRefData/ASD>.<sup>b</sup> All lifetimes taken from [14] except that for level 26524.02 cm<sup>-1</sup> [13].<sup>c</sup> Biémont *et al* [13].<sup>d</sup> Ivarsson *et al* [12].<sup>e</sup> Goly *et al* [11].<sup>f</sup> Lage and Whaling *et al* [8].<sup>g</sup> Blended line in this work. $\bar{\Delta}_{gA}$  and its standard deviation, where

$$\Delta_{g_{ul} A_{ul}} \equiv \frac{(g_{ul} A_{ul})_{\text{ref}} - (g_{ul} A_{ul})_{\text{this work}}}{\sqrt{(\sigma_{ul}^2)_{\text{ref}} + (\sigma_{ul}^2)_{\text{this work}}}}. \quad (3)$$

Since the measured lifetimes used in these references can be quite different, we have also listed the same statistics using  $(g_{ul} A_{ul})_{\text{ref}}$  calculated with our own measured lifetimes, effectively providing a comparison of measured BFs. Table 3 shows very good overall agreement, especially when the

**Table 3.** Overall comparisons of  $gA$  data with other work that used both measured lifetimes and measured BFs.

Reference	$\Delta_{gA}^a$	$\Delta_{gA}^b$
Ivarsson <i>et al</i> [12]	0.30(48)	-0.08(48)
Goly <i>et al</i> [11]	-1.46(30)	-0.11(28)

<sup>a</sup>Calculated using lifetimes from the reference of column 1

<sup>b</sup>Calculated using our lifetimes from [14].

same lifetimes are used for the comparison. There are however individual exceptions, as described above. In a comparison of our results with those of Lage and Whaling [8], where only general statements about error are given, we find that the percentage difference ranges from +39 to -178%, with a standard deviation of 51%. Comparison of our results with those of Biémont *et al* [13] is difficult because their data depends on theoretical branching ratios for which no uncertainty estimates are given. If we take an uncertainty of 50%, based on an upper limit in earlier work [19] by this group, and eliminate three cases where we report blended lines, we find seven cases out of 40 where the  $\Delta$  parameter (defined above) is greater than 2. In five of these transitions, the lines are weak, and for the transition at 396.525 nm,  $\Delta$  is only slightly more than 2. The large disagreement for the transition at 397.214 nm is puzzling since weaker transitions from the same upper level ( $25610.20\text{ cm}^{-1}$ ) are in much better agreement.

The Einstein coefficients  $A_{ul}$  and absorption oscillator strengths  $f_{lu}$  were calculated using our previously determined radiative lifetimes [14] and well-known formulae [20] for electric dipole transitions,

$$A_{ul} = R_{ul}/\tau_u, \quad (4)$$

$$g_l f_{lu} = \frac{1}{0.66702\sigma_{ul}^2} g_u A_{ul}, \quad (5)$$

where  $\tau_u$  is the upper-state lifetime,  $g_u = 2J_u + 1$  and  $g_l = 2J_l + 1$  are the statistical weights of the upper and lower levels respectively and  $\sigma_{ul}$  is the transition wave number ( $\text{cm}^{-1}$ ).

## 5. Conclusions

We have measured 260 oscillator strengths for Pr II transitions over the wavelength range 250–850 nm, originating from 32 levels in the range  $\sim 21\,500\text{--}29\,000\text{ cm}^{-1}$ . Highly selective laser excitation of only a single upper level produces an uncluttered fluorescence spectrum, removing any ambiguity in the assignment of a transition to a pair of energy

levels. The oscillator strengths were obtained by combining measured relative intensities with previously measured radiative lifetimes. Of the 260 measured oscillator strengths, 183 have been determined accurately for the first time. The uncertainties arose principally from systematics of the efficiency calibration of the optical detection system (7.1%), with smaller statistical contributions (1.5%). The measured values were compared with prior measurements using both our lifetimes and lifetimes measured by others.

## Acknowledgment

We are grateful to the Natural Sciences and Engineering Research Council of Canada for financial support.

## References

- [1] Wahlgren G M 2002 *Phys. Scr. T* **100** 22
- [2] Burris D L, Pilachowski C A, Armandroff T E, Sneden C, Cowan J J and Roe H 2000 *Astrophys. J.* **544** 302
- [3] Strasser S, Landstreet J D and Mathys G 2001 *Astron. Astrophys.* **378** 153
- [4] Grevesse N and Sauval A J 1998 *Space Sci. Rev.* **85** 161
- [5] Meggers W F, Corliss C H and Scribner B F 1961 *Tables of Spectral-Line Intensities, NBS Monograph 32, Parts I and II* (Washington, DC: US Government Printing Office)
- [6] Meggers W F, Corliss C H and Scribner B F 1975 *Tables of Spectral-Line Intensities, NBS Monograph 145, Parts I and II* (Washington, DC: US Government Printing Office)
- [7] Corliss C H and Bozman W R 1962 *Experimental Transition Probabilities for Spectral Lines of Seventy Elements, Monograph 53* (Washington, DC: US National Bureau of Standards)
- [8] Lage C S and Whaling W 1976 *J. Quant. Spectrosc. Radiat. Transfer* **16** 537
- [9] Andersen T and Sorensen G 1974 *Sol. Phys.* **38** 343
- [10] Kurucz R L and Bell B 1995 *Atomic Line Data, Kurucz CD-ROM No. 23* (Cambridge, MA: Smithsonian Astrophysical Observatory)
- [11] Goly A, Kusz J, Nguyen Quang B and Weniger S 1991 *J. Quant. Spectrosc. Radiat. Transfer* **45** 157
- [12] Ivarsson S, Litzén U and Wahlgren G M 2001 *Phys. Scr.* **64** 455
- [13] Biémont E, Lefèvre P-H, Quinet P, Svanberg S and Xu H L 2003 *Eur. Phys. J. D* **27** 33
- [14] Scholl T J, Holt R A, Masterman D, Rivest R C, Rosner S D and Sharikova A 2002 *Can. J. Phys.* **80** 713
- [15] Kaufman S L 1976 *Opt. Commun.* **17** 309
- [16] Hall J L and Lee S A 1976 *Appl. Phys. Lett.* **29** 367
- [17] Cadwell L H 1996 *Am. J. Phys.* **64** 917
- [18] Rehse S J, Li R, Scholl T J, Sharikova A, Chatelain R, Holt R A and Rosner S D 2006 *Can. J. Phys.* **84** 723
- [19] Xu H L, Svanberg S, Quinet P, Garnir H P and Biémont E 2003 *J. Phys. B: At. Mol. Opt. Phys.* **36** 4773
- [20] Martin W C and Wiese W L 1996 *Atomic, Molecular, and Optical Physics Handbook* ed Drake G W F (New York: AIP)